06

Plasma dynamic synthesis of nanodispersed cubic tungsten oxide in a carbon dioxide environment

© I.I. Shanenkov, D.S. Nikitin, A. Nassyrbayev, Yu.L. Shanenkova, A.A. Sivkov

Tomsk Polytechnic University, Tomsk, Russia
E-mail: nikitindmsr@yandex.ru

Received June 25, 2025
Revised August 1, 2025
Accepted August 11, 2025

A nanodispersed W−O powder was successfully synthesized in a pulsed arc discharge plasma flowing into a gaseous CO_2 environment. The resulting product is characterized by the presence of a metastable, cubic modification of c-WO_3, the existence of which in natural conditions has been controversial until now. Examination of the product using XRD analysis and transmission electron microscopy revealed that it contains ~ 90 by mass of the c-WO_3 crystalline phase in the form of nanoscale particles.

Keywords: plasma, arc discharge, tungsten oxide, nanopowders.

DOI: 10.61011/TPL.2025.11.62208.20417

With recent developments in nanotechnology, the interest in tungsten oxide WO_3 has increased significantly, since its properties are improved substantially in the nanodimensional form. Owing to this refinement of parameters at the nanoscale, it is used in a number of promising areas: photo- and electrocatalysis, solar power engineering, and fabrication of electrochromic devices and gas sensors [1–3]. The specific features of W−O bonding allow for the formation of several polymorphic modifications of WO_3, which include monoclinic II (ε-WO_3), triclinic (δ-WO_3), monoclinic I (γ-WO_3), orthorhombic (β-WO_3), tetragonal (α-WO_3), and cubic (c-WO_3) ones; notably, phase transformations depend on temperature and are normally reversible, making the δ- and γ-modifications the most commonly encountered in nature [4].

Cubic modification c-WO_3 stands out among tungsten oxides as a metastable crystalline phase the possibility of existence of which in natural conditions has long remained debatable [5]. Although the detection of this polymorphic modification by X-ray diffractometry has been reported in experiments on high-temperature heating of tungsten-containing acids [6–9], successful stabilization of the cubic phase at room temperature in stoichiometric (c-WO_3) and non-stoichiometric (c-WO_{3-x}) forms has been demonstrated in a very limited number of studies [5,10]. Both processes are characterized by the use of inert or reaction-neutral gases (Ar, H_2).

c-WO_3 is hard to stabilize under natural conditions due to the narrowness of the temperature range of its existence and thermodynamic instability, which is characterized by phase transition c-$WO_3 \rightarrow \gamma$-WO_3 under a static slow temperature reduction. It is theoretically possible to synthesize such metastable compounds under the conditions of ultrafast crystallization (e.g., when a pulsed high-speed electroerosive plasma jet is cooled), which has already been demonstrated successfully in a plasma dynamic synthesis system for a different tungsten-containing material (cubic tungsten carbide WC_{1-x}) [11].

In the present study, we propose a new method for forming a metastable crystalline modification of tungsten oxide by plasma dynamic synthesis in a carbon dioxide (mild oxidizing agent) environment. The method relies on the use of high-speed electric discharge plasma generated by a coaxial magnetoplasma accelerator with a tungsten electrode system. The central electrode (a VA tungsten alloy cylinder with a diameter of 10 mm and a length of 12 mm) and the barrel electrode (a VA tungsten alloy pipe with an outer diameter of 25 mm, an inner diameter of 12 mm, and a length of 140 mm) are positioned coaxially, forming a cylindrical interelectrode space (8 mm in diameter, 9.5 mm in length) bounded by a glass-fiber laminate insulator, where the plasma structure is formed. The accelerator is powered in the single-pulse mode by a capacitive energy storage device. When a potential difference from the capacitive energy storage device with capacitor bank capacitance $C = 14.4$ mF and charging voltage $U_C = 2.5$ kV is applied between the central electrode and the barrel electrode, an arc discharge characterized by a current of 130 ± 5 kA and a power of 122 ± 5 MW is initiated. The resulting plasma structure moves along the acceleration channel and causes electroerosion of the electrode system, drawing liquid-phase material and tungsten macroparticles into the reaction zone. The high-energy (26 ± 2 kJ) pulsed ($450 \pm 10\,\mu$s) impact of a plasma jet accelerated to several km/s [12,13] on the gaseous atmosphere in the reactor chamber, which is filled with carbon dioxide (GOST 8050−85, more than 99.5 % CO_2) under a pressure of 2 atm, induces decomposition of CO_2 molecules with the formation of free oxygen radicals, which may react with eroded tungsten through oxidation reactions at elevated pressure and temperature levels in the leading-edge shock wave of the plasma jet. The gas composition in the reactor chamber was monitored

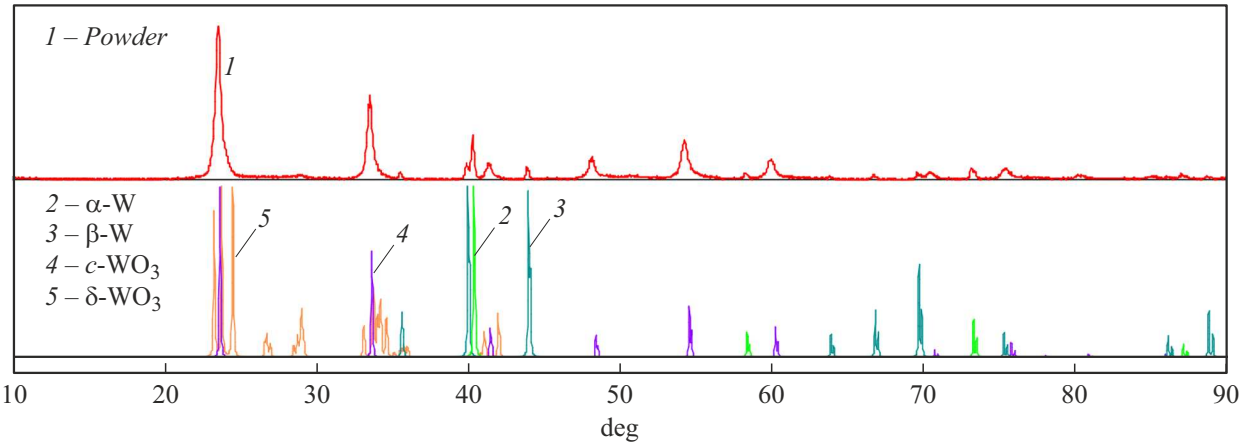

Figure 1. X-ray diffraction pattern of the synthesized product in the W−O system.

by taking gas samples from the working chamber volume and analyzing them with a Chromatec-Crystal 5000.2 gas chromatograph (Chromatec, Russia). The degree of carbon dioxide conversion, which is characterized by the difference in gas content measured by the gas analyzer before and after the experiment, was as high as 0.5 %.

Highly dispersed crystals form in the reactor chamber from the liquid and vapor phases of the synthesized oxidized material as a result of homogeneous nucleation under intense cooling (up to 10^6-10^7 K/s). This may be followed by secondary processes of product particle growth as a result of heterogeneous condensation, as well as coagulation and agglomeration of crystalline objects. Following the deposition of nanodispersed particles on the walls of the reactor chamber, the powdered product is collected manually. The powder mass is ~ 1 g, and the specific energy consumption in the process is ~ 45 kJ/g (0.0125 kW · h/g).

The phase composition of the dispersed material obtained by plasma dynamic synthesis was studied by X-ray diffractometry (Shimadzu XRD-7000; CuK_α radiation; $\lambda = 1.5406$ Å; scanning rate, 2 deg/min; step, 0.03 deg; exposure time, 1 s). The X-ray diffraction pattern of the powdered product is shown in Fig. 1. Judging by the nature of intensity maxima, the product is heterophase and cubic tungsten trioxide c-WO_3 (ICDD 04-004-5867, Pm-3m, N 221, $a = 3.8380$ Å) is dominant in it. The main intensity peaks of the c-WO_3 phase in the powder diffraction pattern are shifted slightly relative to their reference positions, which suggests the formation of a non-stoichiometric compound with an oxygen deficiency (WO_{3-x}). This is quite probable both for the W−O system with a wide homogeneity range (primarily $2 \leqslant 3 - x \leqslant 3$) [14] and for the specific cubic crystalline phase, which is normally characterized by a certain oxygen deficiency ($2.9 \leqslant 3 - x \leqslant 3$) [5].

In addition to tungsten oxide, the product contains two modifications of elemental tungsten: the stable cubic α-phase (ICDD 00-004-0806, $Im3m$, N 229, $a = 3.1648$ Å) and the metastable cubic β-phase (ICDD 00-047-1319, $Pm3n$, N 223, $a = 5.0500$ Å). The low-intensity reflections located at $2\theta \approx 28.8$ deg also reveal the presence of trace amounts of a more stable triclinic δ-modification WO_3 (ICDD 00-032-1395, P-1, N 2).

Quantitative X-ray diffraction analysis was performed using the Rietveld method (Table 1). The c-WO_3 content was found to be greater than 90 mass%. The analyzed product composition suggests that electroerosion of the tungsten electrode system with subsequent release of reactive tungsten, which is largely oxidized to form WO_3 and crystallizes predominantly in the metastable cubic phase, proceeds in the course of plasma treatment. A fraction of tungsten remains in an unoxidized form in two W modifications. It should be noted that the formation of metastable c-WO_3 was made possible by the setting of specific levels of intensity and duration of high-temperature exposure, since the W−O system is too sensitive to the magnitudes, gradients, and rates of temperature change. In the few experimental studies available, stabilization of the cubic phase of tungsten oxide is typically attributed to the formation of oxygen vacancies with the probable coexistence of several types of metal cations in the crystal structure: W^{6+} (dominant type), W^{5+}, and W^{4+} [5].

The microstructure of the synthesized dispersed material was characterized by scanning electron microscopy (SEM) (Tescan Mira 3LMU with an energy-dispersive X-ray microanalysis system; accelerating voltage, up to 30 kV; ultimate resolution, 1.8 nm) and transmission electron microscopy (TEM) (JEOL JEM 2100F; accelerating voltage, up to 200 kV; ultimate resolution, 0.14 nm). Figure 2, *a*

Table 1. Estimated content of crystalline phases (in mass%) in the composition of the synthesis product

α-W	β-W	c-WO_3	δ-WO_3
7 ± 1	3 ± 1	91 ± 2	–

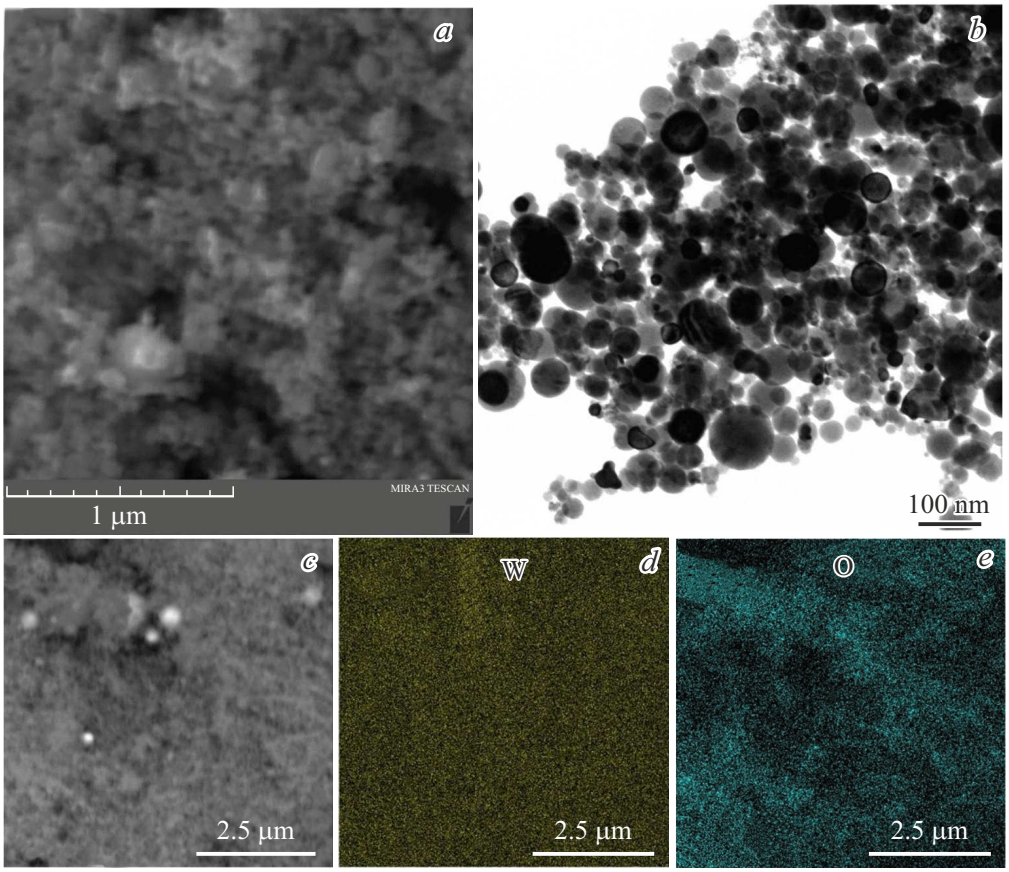

Figure 2. SEM image (*a*); TEM image (*b*); results of EDS mapping of a cluster of synthesized product particles: the original micrograph (*c*) and distribution maps for tungsten (*d*) and oxygen (*e*).

shows the SEM image of the obtained powder. The product is fairly uniform in terms of particle size and object contrast. The material is composed primarily of highly dispersed particles (no larger than $1\,\mu$m in size) that are bonded together in both loose and dense agglomerates. Larger particles are few in number and reach several micrometers in diameter; they are also characterized by a higher contrast, which suggests that they should be identified as high-density tungsten. The highly dispersed structure of the product obtained in the W–O system distinguishes it from materials that were synthesized by the plasma dynamic method in systems with other metal (e.g., titanium) electrodes and are characterized by the presence of large spherical particles up to several tens of micrometers in size [12,13]. This significant change in the particle size distribution is apparently attributable to the specific properties of tungsten: its high melting point (3422 °C) and work function (4.54 eV), which affect the process of electroerosion of the material.

According to the results of energy-dispersive spectroscopy (EDS) analysis of the product (Table 2), the synthesized powder is composed primarily of tungsten and oxygen, while the amount of impurities (Ca, Ti, La) is minimal. As expected, the atomic content of oxygen exceeds significantly the tungsten content. Figures 2, *d* and *e* present the distribution maps of elemental W and O superimposed on the original micrograph (Fig. 2, *c*). It is evident that the distributions of both tungsten and oxygen are uniform, which verifies the formation of a single compound in the form of tungsten oxide within the product and its constituent particles.

The structure of the synthesized material at the nanoscale was studied using high-resolution TEM methods. Figure 2, *b* shows a typical TEM image of the cluster that is indicative of the formation of a nanostructure in the product. The powder consists primarily of spherical particles up to

Table 2. Quantitative elemental analysis of the synthesis product

Element	Content	
	mass%	at.%
O	14.43	65.67
Ca	0.15	0.27
Ti	0.17	0.26
La	0.53	0.28
W	84.72	33.52
Total	100.00	100.00

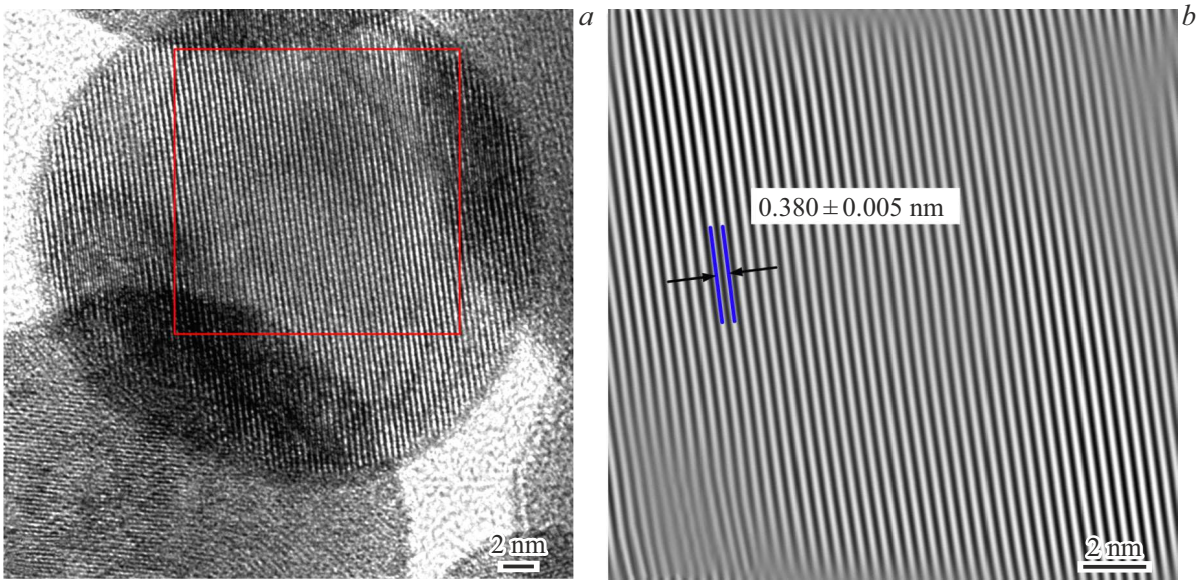

Figure 3. High-resolution TEM images of the synthesized product: bright-field image (a) and direct-resolution IFFT image of the indicated region (b).

100 nm in size (the average particle size is ~ 30 nm). It was hard to identify any significant differences in the morphology of formed particles; however, objects classified definitively as cubic tungsten oxide c-WO_3 were revealed. Figure 3, a shows a typical spherical single-crystal nanoparticle ~ 20 nm in size without a shell. The TEM data were subjected to inverse Fourier transform (in Gatan Digital Micrograph 1.80.70) to obtain an image with resolved atomic planes (Fig. 3, b). The calculated interplanar spacing of 0.380 ± 0.005 nm corresponds to the reference values ($d_{200} = 0.37610$ nm) for the cubic tungsten oxide phase.

Thus, the plasma dynamic method allows for highly efficient synthesis of cubic tungsten oxide c-WO_3. The generation of an arc discharge and a plasma jet using a coaxial magnetoplasma accelerator with tungsten electrodes induces electroerosion of metal from the surface of the electrode system, CO_2 decomposition in the reactor chamber under high-intensity exposure, and oxidation of tungsten by the produced free oxygen radicals. A highly dispersed product dominated by the c-WO_3 crystalline phase is synthesized as a result. Nanoparticles in the formed material are spherical and single-crystal with an average size of ~ 30 nm.

Funding

This study was supported by the Russian Science Foundation, grant № 24-79-10113 (https://rscf.ru/en/project/24-79-10113/).

Conflict of interest

The authors declare that they have no conflict of interest.

References

[1] S. Zhou, Z. Yang, X. Feng, J. Zuo, N. Wang, K. Thummavichai, Y. Zhu, iScience, **27** (4), 109535 (2024). DOI: 10.1016/j.isci.2024.109535
[2] X. Gu, S. Lin, K. Qi, Y. Yan, R. Li, V. Popkov, O. Almjasheva, Sep. Purif. Technol., **345**, 127299 (2024). DOI: 10.1016/j.seppur.2024.127299
[3] X. Li, L. Fu, H. Karimi-Maleh, F. Chen, S. Zhao, Heliyon, **10** (6), e27740 (2024). DOI: 10.1016/j.heliyon.2024.e27740
[4] H. Zheng, J.Z. Ou, M.S. Strano, R.B. Kaner, A. Mitchell, K. Kalantar-Zadeh, Adv. Funct. Mater., **21** (12), 2175 (2011). DOI: 10.1002/adfm.201002477
[5] Z. Fang, S. Jiao, B. Wang, W. Yin, S. Liu, R. Gao, Z. Liu, G. Pang, S. Feng, Mater. Today Energy, **6**, 146 (2017). DOI: 10.1016/j.mtener.2017.09.014
[6] O. Yamaguchi, D. Tomihisa, H. Kawabata, K. Shimizu, J. Am. Chem. Soc., **70**, C94 (1987). DOI: 10.1111/j.1151-2916.1987.tb05010.x
[7] A.R. Siedle, T.E. Wood, M.L. Brostrom, D.C. Koskenmaki, B. Montez, E. Oldfield, J. Am. Chem. Soc., **111**, 1665 (1989). DOI: 10.1021/ja00187a019
[8] C. Guéry, C. Choquet, F. Dujeancourt, J.M. Tarascon, J.C. Lassegues, J. Solid State Electrochem., **1**, 199 (1997). DOI: 10.1007/s100080050049
[9] C. Balazsi, M. Farkas-Jahnke, I. Kotsis, L. Petrás, J. Pfeifer, Solid State Ionics, **141**, 411 (2001). DOI: 10.1016/S0167-2738(01)00806-2
[10] P.H. Sung, H.K. Yen, S.M. Yang, K.C. Lu, Nanomaterials, **13** (7), 1197 (2003). DOI: 10.3390/nano13071197
[11] I. Shanenkov, D. Nikitin, A. Ivashutenko, Y. Shanenkova, Y. Vympina, D. Butenko, W. Han, A. Sivkov, Ceram. Int., **47** (5), 6884 (2021). DOI: 10.1016/J.CERAMINT.2020.11.035

[12] A. Sivkov, E. Naiden, A. Ivashutenko, I. Shanenkov, J. Magn. Magn. Mater., **405**, 158 (2016). DOI: 10.1016/j.jmmm.2015.12.072
[13] A. Sivkov, Y. Vympina, A. Ivashutenko, I. Rakhmatullin, Y. Shanenkova, D. Nikitin, I. Shanenkov, Ceram. Int., **48** (8), 10862 (2022). DOI: 10.1016/j.ceramint.2021.12.303
[14] B. Wang, X. Zhong, H. Xu, Y. Zhang, U. Cvelbar, K. Ostrikov, Micromachines, **13** (12), 2075 (2022). DOI: 10.3390/mi13122075

Translated by D.Safin